Article

The Influence of Different Dynamic Material Constitutive Models on the Impact Performance of Circular CFST Columns

Xi-Feng Yan [1,2] , **Siqi Lin** [3,*] **and Mizan Ahmed** [4]

1   School of Civil Engineering, Xi'an University of Architecture and Technology, Xi'an 710055, China;
     yan-xf@xauat.edu.cn
2   Key Lab of Structural Engineering and Earthquake Resistance, Ministry of Education (XAUAT),
     Xi'an 710055, China
3   Key Laboratory of Urban Security and Disaster Engineering of Ministry of Education,
     Beijing University of Technology, Beijing 100124, China
4   School of Civil and Mechanical Engineering, Curtin University, Kent Street, Bentley, WA 6102, Australia;
     mizan.ahmed@curtin.edu.au
*   Correspondence: lsq8986@bjut.edu.cn

Abstract: At present, there is a lack of research on the influence of different dynamic constitutive models of steel and concrete on the dynamic mechanical properties of concrete-filled steel tubular (CFST) columns under lateral impact. In this paper, A comprehensive numerical study on the effects of different dynamic constitutive models of steel and concrete on the lateral impact response of CFST columns was conducted. The dynamic constitutive models of steel and concrete with different strengths were divided into four categories, namely, normal-strength steel, high-strength steel, normal-strength concrete and high-strength concrete. The established finite element model of CFST columns considering the progressive damage degradation of steel as well as the compressive and tensile damage factors of concrete was verified against published experimental data. Based on the verified FE model, the effects of different dynamic constitutive models of steel and concrete on the impact response of circular CFST columns were analyzed. The analyzed results show that the different dynamic constitutive models of steel have different effects on the impact force and mid-span time-history deflection curves of CFST columns. The analysis result, ignoring the effect of concrete strain rate, is in good agreement with the CEB-FIP model considering the effect of steel strain rate. This is because the largest proportion of the impact energy of CFST members is mainly assimilated by the outer steel tube.

Keywords: concrete-filled steel tubes; dynamic constitutive model; lateral impact; finite element model

1. Introduction

Impact is one of the three major disasters (fire, earthquake and impact) that leads to the damage and even collapse of civil engineering structures. Impact effects include car, ship and plane collisions; the accidental fall of elevators, billboards, temporary construction facilities and other construction equipment or attachments; secondary disasters caused by earthquakes, fires, mountain torrents and mudslides; and even terrorist attacks. As a result, impact effects have the distinctive characteristics of low frequency and high hazard, and are an accidental effect that must be considered for most major civil engineering structures, crash-prone structures, crash-proof enclosures, national defense structures, and anti-explosion and anti-terror facilities [1–5]. In particular, accidents such as vehicle collisions, ship collisions and terrorist attacks occur frequently (see Figure 1); therefore, more attention is being drawn toward investigating the impact resistance performance of important architectural structures and components.
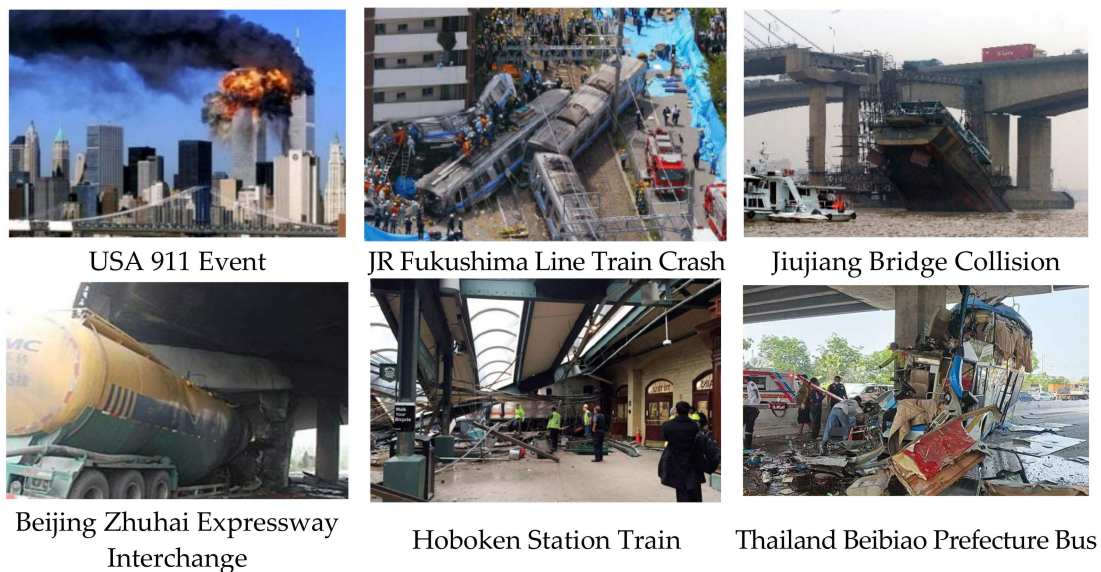
USA 911 Event   JR Fukushima Line Train Crash   Jiujiang Bridge Collision

Beijing Zhuhai Expressway Interchange   Hoboken Station Train   Thailand Beibiao Prefecture Bus

Figure 1. Cases of actual engineering impact accidents.

Concrete-filled steel tubes (CFSTs) have been widely used in various modern building structures owing to their outstanding properties such as high bearing capacity, good ductility and stiffness, simple construction, excellent seismic performance, and good fire resistance. Owing to their good mechanical properties, CFST columns are widely used in bridges and high-rise buildings [6–9]. Consequently, CFST columns constantly suffer from low-speed impact load during practical engineering service, mainly including vehicle collision, wave impact, etc. CFST columns are often used as primary load-bearing structural components, which may cause damage or even a collapse of the structure due to lateral impact, causing serious damage to structures and potential loss of life [10]. Therefore, it is of great significance to carry out research on the lateral impact response of CFST columns.

Previously, researchers carried out experimental research, numerical simulations and theoretical analyses on the lateral impact response of CFST members [11–15]. Wang et al. [11], by conducting experimental research and numerical analyses, ascertained the influence of different steel tube wall thicknesses, boundary conditions and axial loads on the impact response of circular CFST members. According to the test and numerical analysis results, a functional relationship between the confinement coefficient and the critical impact energy of CFST members was established. Qu et al. [16] developed a simplified analysis method for the impact behavior of fixed, simply supported CFST columns in combination with test and numerical analysis results that well predicts the maximum deflection of CFST columns. Yousuf et al. [17,18] performed experimental and numerical studies of stainless CFST members under static and impact loads. The results showed that the impact position at one-fourth of the column height can bear a greater load and produce a smaller deflection than that at the mid-span. Han et al. [19] experimentally and numerically evaluated the effects of material strain rate and inertia force on the impact response of high-strength concrete CFST columns, and the flexural capacity model of CFSTs under impact load was further simplified. Cai et al. [20], through finite element analysis, found that the deformation of the impact part became more obvious as the impact height and slenderness ratio were enhanced. Based on the numerical analysis results, a calculation model for predicting the dynamic bearing capacity coefficient of CFST members was established. Yang et al. [21], based on the drop weight impact test, found that high-strength concrete-filled CFST members have good impact resistance similar to normal-strength ones, in addition to high impact force platform values and small deflection.

Overall, it can be observed from the above research that a lot of work has been conducted on the lateral impact response of CFST members. However, the research parameters have mainly been focused on the axial compression load ratio, concrete strength, section

shape, steel yield strength, steel ratio and column span-depth ratio, while research on the differences between steel and concrete dynamic constitutive models under impact loads is very limited. The differences in material dynamic constitutive models will bring great deviation to the analysis results of the dynamic mechanical properties of CFST members under lateral impact [22]. However, there is a lack of research on the influence of different steel and concrete dynamic constitutive models on the dynamic mechanical properties of CFST members. Therefore, it is urgent to study the influence of different dynamic constitutive models of steel and concrete on the mechanical properties of CFST members.

The influence of the differences in dynamic mechanical constitutive models of different materials with different strengths on the impact response of CFST members, in this paper, is comprehensively investigated. The classification of different materials with different strengths is divided into four categories, namely, normal-strength steel, high-strength steel, normal-strength concrete and high-strength concrete. By the finite element (FE) method, the effects of different steel and concrete dynamic constitutive models on the lateral impact response of circular CFST columns are analyzed. At the same time, the progressive damage degradation of steel, as well as the compressive and tensile damage factors of concrete, are introduced.

2. Finite Element Modeling

2.1. General

Overall, two types of analysis software, LS-DYNA and ABAQUS, are commonly used in impact analysis [2,11]. LS-DYNA is a well-known universal display dynamic analysis program that is particularly suitable for solving nonlinear dynamic impact problems such as high-speed collisions, explosions and metal forming of various nonlinear structures. This manuscript mainly focuses on low-speed impact issues, which can be well addressed by ABAQUS. ABAQUS has two main analysis modules: ABAQUS/Standard provides universal analysis capabilities, such as stress and deformation, heat exchange, mass transfer, etc. The ABAQUS/Explicit application provides a powerful tool for solving complex contact problems by displaying and integrating time, and is suitable for analyzing transient dynamic events. This study includes implicit (simulation of axial load) and explicit analyses. Therefore, ABAQUS is suitable as the application is very advanced in stress-strain analysis. The validation research of ABAQUS in this article lays a certain foundation for the subsequent research of the authors.

Based on ABAQUS finite element software [23], an FE model of CFST columns under lateral impact load was developed. This model took into account the strain rate effect of steel and concrete materials, the influence of the steel tube fracture failure model and the compression and tension damage factors of concrete. The accuracy and reliability of the FE model were compared and verified with previous experimental results.

2.2. Material Model of Structural Steel

An ideal multilinear stress versus strain constitutive relation given by Han et al. [24] was applied to simulate steel, as illustrated in Figure 2. This model has been widely adopted by researchers previously, e.g., Yan et al. [9], Deng et al. [10], Zhao et al. [14], etc. The stress versus strain constitutive relation of steel proposed by Han et al. [24] is as follows:

$$\sigma_s = \begin{cases} E_s \varepsilon & \varepsilon \leq \varepsilon_1 \\ -A\varepsilon^2 + B\varepsilon + C & \varepsilon_1 \leq \varepsilon \leq \varepsilon_2 \\ f_{sy} & \varepsilon_2 \leq \varepsilon \leq \varepsilon_3 \\ f_{sy}\left[1 + 0.6\frac{\varepsilon - \varepsilon_3}{\varepsilon_4 - \varepsilon_3}\right] & \varepsilon_3 \leq \varepsilon \leq \varepsilon_4 \\ 1.6 f_{sy} & \varepsilon \geq \varepsilon_4 \end{cases} \tag{1}$$

where E_s and f_{sy} represent the modulus of elasticity and yield strength of the steel used, respectively, and E_s is equal to 2.0×10^5 MPa; $A = 0.2 f_{sy}/(\varepsilon_2 - \varepsilon_1)^2$, $B = 0.2 A \varepsilon_2$, $C = 0.8 f_{sy} + A \varepsilon_1^2 - B \varepsilon_1$, $\varepsilon_1 = 0.8 f_{sy}/E_s$, $\varepsilon_2 = 1.5 \varepsilon_1$, $\varepsilon_3 = 10 \varepsilon_2$, $\varepsilon_4 = 100 \varepsilon_2$.
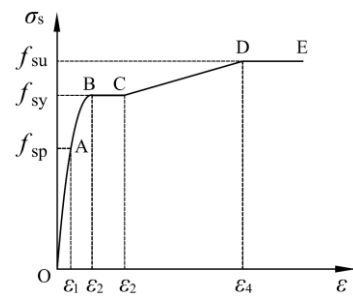
Figure 2. Stress (σ)–strain (ε) relationship for steel.

It is worth noting that the engineering stress–strain relationship of steel must be converted to the real stress–strain relationship, which can then be input into the numerical model of ABAQUS. The conversion formulas are as follows:

$$\sigma_{\text{true}} = \sigma_{\text{eng}}(1 + \varepsilon_{\text{eng}}) \tag{2}$$

$$\varepsilon_{\text{true}} = \ln(1 + \varepsilon_{\text{eng}}) \tag{3}$$

where σ_{eng} and ε_{eng} are the engineering stress and strain, respectively; σ_{true} and $\varepsilon_{\text{true}}$ are the actual stress and strain, respectively.

In addition, in order to simulate the cracking of steel tubes, a steel damage model as depicted in Figure 11 of reference [1], was introduced into the steel constitutive relation by entering key parameters in the interface of the steel material properties subroutine. As the steel strain accesses the critical point of the equivalent plastic strain $\bar{\varepsilon}_0^{\text{pl}}$, the steel begins to be in the evolution phase of plastic damage. The descending part of the curve (CD segment) represents the degree of damage evolution of steel under different plastic strains. Here, D_{ic} is the damage evolution factor, which is used to control the damage evolution path of steel. When D_{ic} equals 0, this indicates the beginning of damage. At the same time, when D_{ic} equals 1, this represents the complete cracking of the steel.

In order to lower the effect of the steel mesh on the results of damage evolution, in this paper, a damage evolution criterion based on the equivalent plastic displacement was adopted. Based on the equivalent plastic strain $\bar{u}_{\text{f}}^{\text{pl}}$ and the characteristic length L_{c} of the element, as the damage criteria were met, the equivalent plastic displacement $\bar{u}_{\text{f}}^{\text{pl}}$ at complete cracking was obtained and expressed as $\bar{u}_{\text{f}}^{\text{pl}} = L_{\text{c}}\bar{\varepsilon}_{\text{f}}^{\text{pl}}$. L_{c} herein is the specific value of the volume of the minimum element divided by its largest area, and the value of L_{c} adopts 10 mm in line with the mesh dimension of the FE model.

2.3. Material Model of Concrete

The stress versus strain constitutive relation of concrete proposed by Han et al. [24] achieved excellent performance simulation of CFST columns under different loading conditions, such as compression, flexure, and combined compression and bending. Therefore, in this current paper, the stress versus strain constitutive relation of concrete proposed by Han et al. [24] was employed and determined by the following equation:

$$y = \begin{cases} 2x - x^2 & x \le 1 \\ \dfrac{x}{\beta_0(x-1)^{\eta} + x} & x > 1 \end{cases} \tag{4}$$

in which $x = \varepsilon/\varepsilon_0$, $y = f/f_{\text{c}}$, f represents the axial stress of concrete when the axial strain reaches ε, f_{c} represents the cylinder concrete strength and the corresponding strain is ε_0; η and β_0 denote the parameters that are decided by the form of the column cross-section. H is

equal to 2 for the circular cross-section and the corresponding parameter β_0 is determined by the following equation:

$$\beta_0 = 0.5\left(2.36 \times 10^{-5}\right)^{\left[0.25+(\xi-0.5)^7\right]}\left(f_c'\right)^{0.5} \geq 0.12 \tag{5}$$

where ξ denotes the nominal confinement factor and is obtained by $\xi = \left(A_s f_{sy}\right)/\left(A_c f_{ck}\right)$. A_c and A_s represent the cross-section areas of infilled concrete and steel tube, respectively; f_{ck} is the characteristic concrete strength.

In this study, the damage plasticity model of concrete was adopted and introduced into the constitutive relation of concrete. The five key parameters, namely, the dilation angle ψ, the ratio of the second stress invariant of the tensile meridian to that of the compressive meridian K_c, the eccentricity e, the ratio of the biaxial compressive strength to the uniaxial compressive strength f_{bo}/f_c' and the viscosity parameter v needed to be determined. Based on previous studies [6,14], in this study, the values of ψ, K_c, f_{bo}/f_c', e and v were taken as $30°$, 1.16, 0.1, 2/3 and 0.0005, respectively. According to ACI 318 [25], the Young's modulus E_0 and Poisson's ratio v_c of the concrete used were $4730\sqrt{f_c'}$ and 0.2, respectively.

In the process of impact, CFST members may bend and deform, and the tensile softening performance of the concrete in tension should be considered. In this paper, the tensile softening behavior of concrete was defined by the tensile stress vs. strain constitutive relation proposed by Han et al. [24]; its calculation expression is as follows:

$$y = \begin{cases} 1.2x - 0.2x^6 & x \leq 1 \\ \dfrac{x}{0.31\sigma_p^2(x-1)^{1.7} + x} & x > 1 \end{cases} \tag{6}$$

where $x = \varepsilon_c/\varepsilon_p$, $y = \sigma_c/\sigma_p$, $\sigma_p = 0.26(1.25f_c')^{2/3}$ and $\varepsilon_p = 43.1\sigma_p$ $(\mu\varepsilon)$.

In addition, the compressive and tensile damage factors of concrete were added to the constitutive models of concrete. The damage factor of concrete can be determined by the following equation:

$$d_c = \frac{(1-\beta_c)\widetilde{\varepsilon}_c^{in} E_0}{\sigma_c + (1-\beta_c)\widetilde{\varepsilon}_c^{in} E_0} \tag{7}$$

where inelastic strain $\widetilde{\varepsilon}_c^{in} = \varepsilon_c - \sigma_c/E_0$ and β_c is the proportion of plastic strain $\widetilde{\varepsilon}_c^{pl}$ to inelastic strain $\widetilde{\varepsilon}_c^{in}$. The value of β_c is 0.6 for compression and 0.9 for tension in this paper. Moreover, the compression damage recovery factor w_c and tension damage recovery factor w_t are 1 and 0, respectively.

2.4. Material Strain Rate Effect

The structural response under impact and other dynamic loads is different from that under quasi-static loads. Increasing the loading rate usually causes the steel strength to significantly improve. To take into account the strain rate effect in the numerical simulation, the constitutive models of Cowper–Symonds [26] and Johnson–Cook [27] are usually adopted to reflect the increase in steel strength. Compared with the Johnson–Cook constitutive model, the Cowper–Symonds constitutive model exhibits a more concise form and fewer parameters need to be determined. As a result, the Cowper–Symonds constitutive model was adopted in this study:

$$\sigma_d/\sigma_s = 1 + \left(\dot{\varepsilon}_d/D\right)^{1/p} \tag{8}$$

where the values of D and p are 6844 s^{-1} and 3.91, respectively.

Similar to the dynamic mechanical properties of steel, concrete exhibits large and complex strain rate effects under dynamic loading. At present, the empirical formula

provided in the European Concrete Institute Code (CEB-FIP, 1993) [28] can be used to calculate the dynamic increase factor of concrete, as follows:

For compression
$$\begin{cases} f_{cd}/f_{cs} = (\dot{\varepsilon}/\dot{\varepsilon}_{co})^{1.026\alpha_{cs}}, & |\dot{\varepsilon}| \le 30 \text{ s}^{-1} \\ f_{cd}/f_{cs} = \gamma_s (\dot{\varepsilon}/\dot{\varepsilon}_{co})^{1/3}, & |\dot{\varepsilon}| > 30 \text{ s}^{-1} \end{cases} \quad (9)$$

For tension
$$\begin{cases} f_{td}/f_{ts} = (\dot{\varepsilon}/\dot{\varepsilon}_{to})^{1.016\delta_s}, & |\dot{\varepsilon}| \le 30 \text{ s}^{-1} \\ f_{td}/f_{ts} = \beta_s (\dot{\varepsilon}/\dot{\varepsilon}_{to})^{1/3}, & |\dot{\varepsilon}| > 30 \text{ s}^{-1} \end{cases} \quad (10)$$

where $\dot{\varepsilon}_{co} = -30 \times 10^{-6}$ s^{-1}, $\dot{\varepsilon}_{to} = 3 \times 10^{-6}$ s^{-1}, $\alpha_{cs} = \frac{1}{5 + 9\ f_c'/f_{co}}$, $\delta_s = \frac{1}{10 + 6\ f_c'/f_{co}}$, $f_{co} = 10$, $\log\gamma_s = 6.156\alpha_{cs} - 2$ and $\log\beta_s = 7.112\delta_s - 2.33$. In the above formulas, f_{cd} and f_{cs} refer to the dynamic and static concrete compressive strength, respectively; f_{td} and f_{ts} refer to the dynamic and static concrete tensile strength, respectively.

Moreover, in the structural dynamic calculation, the influence of inertia force should be considered. Therefore, the density of each material should be defined in the FE material model. Herein, the density of steel and concrete is 7850 kg/m^3 and 2450 kg/m^3, respectively. This study is in the range of low-speed impact. Researchers have concluded that low-velocity impact has a negligible effect on the elastic modulus and Poisson's ratio [11–16]. In this paper, Poisson's ratio was adopted as 0.3. The elastic modulus of steel was 200 GPa if it was not given in the literature. In addition, this study mainly focuses on the low-velocity impact loads. Therefore, the volumetric strain as a function of the bulk modulus of material under pressure was not taken into account.

2.5. Element Mesh, Boundary and Contact Conditions

The typical mesh of the FE model for circular CFST columns is illustrated in Figure 3. As shown in Figure 3, the eight-node linear brick elements with reduced integration (C3D8R) and shell elements (S4R) were utilized to simulate the infilled concrete and steel tubes [29], and a four-node three-dimensional bilinear rigid body quadrilateral shell element (R3D4) was used to simulate the rigid drop hammer. Based on the size analysis of element mesh, the sizes of concrete and steel were selected as 15 mm. In addition, within 200 mm of the impact point, a finer mesh for the steel tube and concrete was used. For simply-simply, all translational degrees of freedom at both ends of the column were constrained, as well as rotation around the y-axis and z-axis. When no axial force was applied to the column, all degrees of freedom at both ends of the fixed-fixed column were constrained. When an axial force was applied to the column, all degrees of freedom at both ends of the fixed-fixed column were constrained, except that the z-axis on the right of the column could be translated. For the application of axial load, the axial load was first applied to the right end of the column through implicit analysis using a spring element. Then, the results of the implicit analysis were restarted in the next explicit analysis step to achieve the application of axial load on the column. Except for translation in the y-axis, all the translations and rotations of the drop hammer were constrained. The FE model took into account the two types of contact interactions [22]: (I) the contact between the steel tube and core concrete and (II) the contact between the drop hammer and steel tube. Along the normal direction of the contact surface, the Hard contact model was used to define the contact interactions. However, the Coulomb friction model was adopted for the tangent direction of contact types (I) and (II), and the corresponding friction factors were 0.6 and 0.16, respectively.
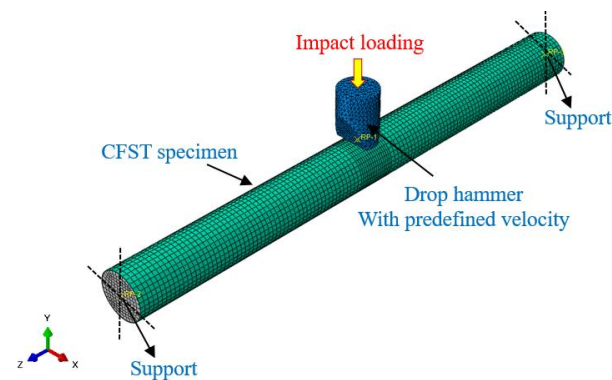
Figure 3. Finite element model.

3. Verification of Numerical Model

A total of 10 specimens collected from published studies [30,31], as listed Table 1, were utilized to check the feasibility of the established FE model. The circular steel tubes were used in all the specimens. The strength grades of steel and concrete were Q235 and C60, respectively. In Table 1, L denotes the length of the test piece, H denotes the impact height, V_0 is the drop velocity at the moment of impact, m_0 is the drop mass, E_0 is the impact energy and n is the axial load ratio of the specimens.

The impact force time-history curves of the test and FEA results for the selected SS2 and CC2 specimens are shown in Figure 4, and the corresponding mid-span deflection time-history curves are illustrated in Figure 5, respectively. From Figures 4 and 5, it can be observed that the established FE model can accurately predict the impact force and mid-span deflection time-history curves of CFST columns under lateral impact. Moreover, a comparison of the platform value of impact force (F_p) and maximum mid-span deflection (u_m) between the test and FEA results are depicted in Figure 6. From Figure 6, it can be found that the mean values of $F_{p,FEA}/F_{p,test}$ and $u_{m,FEA}/u_{m,test}$ are 1.01 and 0.99, respectively, and the corresponding standard deviations of are 0.02 and 0.01, respectively. Overall, the established FE model can accurately predict the lateral impact performance of circular CFST columns and can be used for impact response analysis of CFST members.

Table 1. Details of the published specimens.

| Specimen No.	Boundary Condition	$D \times t$ (mm)	L (mm)	H (m)	V_o (m/s)	m_o (kg)	E_o (m)	n	Ref.
CC1	Fixed-fixed	180 × 3.65	1940	5.5	9.21	465	19.72	0	
CC2	Fixed-fixed	180 × 3.65	1940	2.5	6.40	920	18.84	0	
CC3	Fixed-fixed	180 × 3.65	1940	8.0	9.67	465	21.73	0	
SS1	Simply-simply	180 × 3.65	2800	4.0	8.05	465	15.07	0	[30]
SS2	Simply-simply	180 × 3.65	2800	2.0	5.69	920	14.89	0	
SS3	Simply-simply	180 × 3.65	2800	5.0	8.93	465	18.54	0	
DBF13	Fixed-fixed	114 × 1.7	1200	1.2	4.85	229.8	2.76	0	
DBF17	Fixed-fixed	114 × 1.7	1200	1.0	4.43	229.8	2.30	0	
DBF19	Fixed-fixed	114 × 1.7	1200	1.2	4.85	229.8	2.76	0.3	[31]
DBF21	Fixed-fixed	114 × 1.7	1200	1.0	4.43	229.8	2.30	0.6	
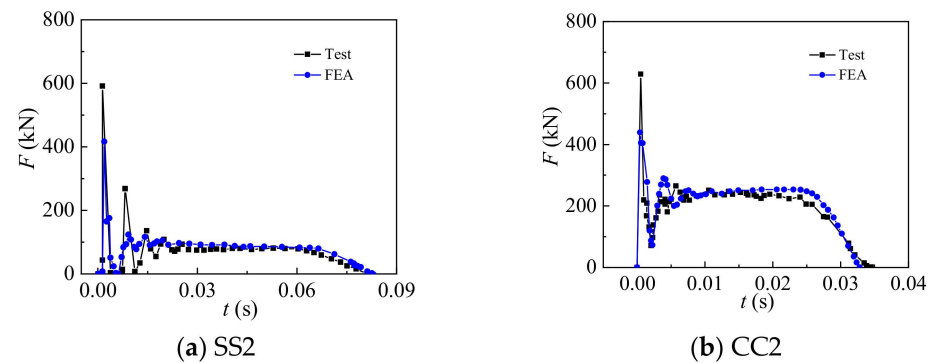
Figure 4. Impact force time-history curves of test and FEA results.
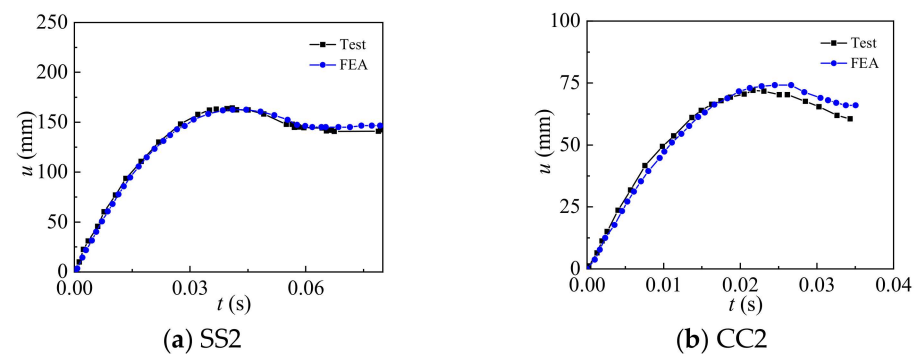

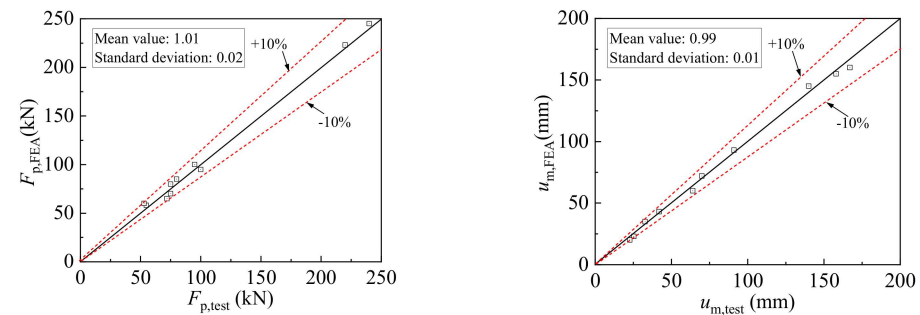**Figure 5.** Mid-span deflection time-history curves of test and FEA results.

Figure 6. Platform value of impact force and maximum mid-span deflection.

4. Parametric Study

The FE model of circular CFST members with simple supports at both ends was established and used to investigate the effects of different dynamic constitutive models of steel and concrete on the lateral impact resistance of CFST columns. The outer diameter and wall thickness of the steel tube were 480 mm and 12 mm, respectively, and the column length was 4000 mm. The steel yield strength f_{sy} was taken as 235 MPa, 355 MPa, 460 MPa and 690 MPa and the concrete strength f_c was taken as 30 MPa, 50 MPa and 70 MPa. In the FE analysis, the section size of the drop hammer with a rigid flat head was 500 mm, with reference to the FAW Jiefang light truck J6F truck. The impact mass was 5000 kg and the corresponding impact speed was 16.67 m/s (60 km/h), where 60 km/h is the general speed limit for urban roads in the city and the minimum speed limit for expressways. The corresponding impact energy was 694 kJ.

In the current research, the C–S and J–C models for steel, the HJC model, and the DIF model proposed by CEB–FIP for concrete were successfully applied in the numerical simulation. Holmquist et al. [33] introduced the influence of strain rate in the Ottosen model

and proposed a rate-dependent damage constitutive model to calculate the large deformation problem of concrete at different strain rates, known as the Holmquist–Johnson–Cook model (HJC model). In this study, the HJC model was introduced in ABAQUS by using the VUMAT subroutine. These models can better reflect the failure phenomenon of steel and concrete under medium or high strain rates. However, compared with high-speed impact problems such as concrete penetration and explosion, the impact of vehicles, ships, falling rocks or waves on CFST members is a low-speed impact problem. The maximum strain rate of components is generally not more than $100\ \mathrm{s}^{-1}$. The material strain rate effect caused by this medium strain rate is also relatively low, making the effect of the dynamic material model on the components not as good as that of high-speed impact. The following is mainly based on ABAQUS to analyze and compare different dynamic constitutive models of materials to quantify the effects of dynamic material constitutive models on the impact response of CFST members. The dynamic constitutive models of several materials analyzed in this paper are shown in Tables 2 and 3.

Table 2. Different dynamic constitutive models of steel.

Steel/Concrete Grade	Cases	Steel Strain Rate Effect Model	Concrete Strain Rate Effect Model
Q235 (Q460)/C30	Case 1	J-C model [26]	CEB-FIP(1993) [28]
	Case 2	C-S model ($D = 40.4\ \mathrm{s}^{-1}$, $p = 5$) [26]	
	Case 3	Ignoring	
	Case 4	Ignoring	Ignoring

Table 3. Different dynamic constitutive models of concrete.

Concrete/Steel Grade	Cases	Concrete Strain Rate Effect Model	Steel Strain Rate Effect Model
C30 (C70)/Q235	Case 1	CEB-FIP(1993) [28]	C-S model ($D = 6844\ \mathrm{s}^{-1}$, $p = 3.91$) [32]
	Case 2	HJC model [33]	
	Case 3	Ignoring	
	Case 4	Ignoring	Ignoring

4.1. Comparison of Different Dynamic Constitutive Models of Steel

For normal-strength and high-strength steel (Q235, Q460), the influence of the difference in dynamic steel constitutive models on the impact force and midspan deflection time-history curves, platform values of impact force and maximum mid-span deflection of CFST members are shown in Figures 7 and 8. From Figures 7 and 8, it can be observed that different steel dynamic constitutive models have significant effects on the impact force and mid-span deflection of CFST columns. In this paper, case 1 was used as the benchmark. From Figure 7, it can be observed that the steel dynamic constitutive models of cases 2 and 3 significantly reduce the platform value of impact force and increase the impact duration, thus increasing mid-span displacement and deformation compared to those of case 1. Because the models in cases 2 and 3 were respectively inclined to elastic dynamic conditions and applied to high strain rates, the impact force of CFST columns was greatly overestimated. The model in case 3 was in good agreement with the model in case 4 regarding the impact process, impact platform section and impact duration change trend; thus, it can well evaluate the impact resistance performance of the component. The simulation results of the case 3 and case 4 models show that these models reduce the impact platform value, prolong the impact duration and increase overall deformation. Because the models in cases 3 and 4 did not consider the strain rate effect of steel, there was no strain rate hardening effect on the impact process. As a result, the impact force of CFST columns was greatly underestimated.
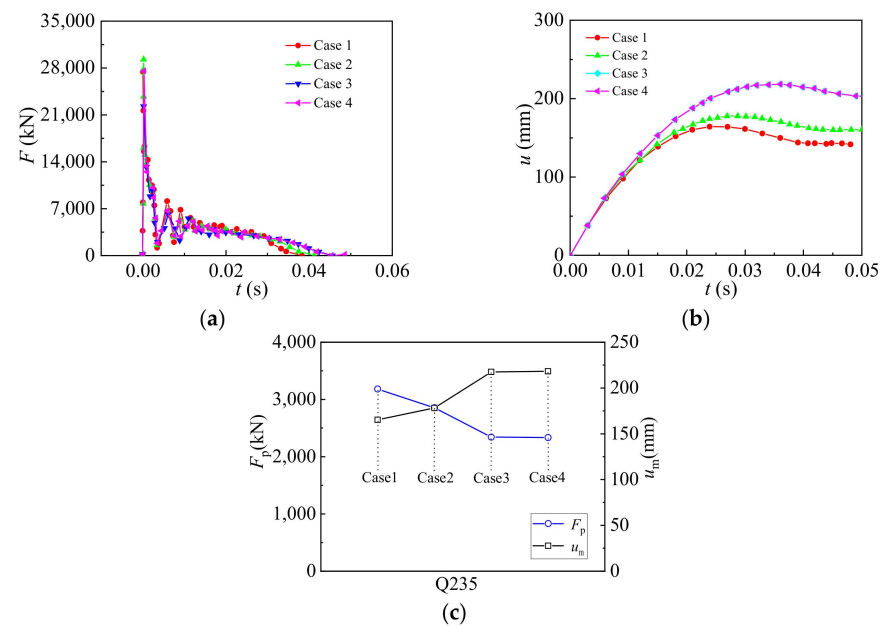
Figure 7. Comparison of Q235 steel with different dynamic constitutive models. (**a**) Comparison of impact force time-history curves of Q235 steel. (**b**) Comparison of mid-span deflection time-history curves of Q235 steel. (**c**) Platform value of impact force and maximum mid-span deflection of Q235 steel.
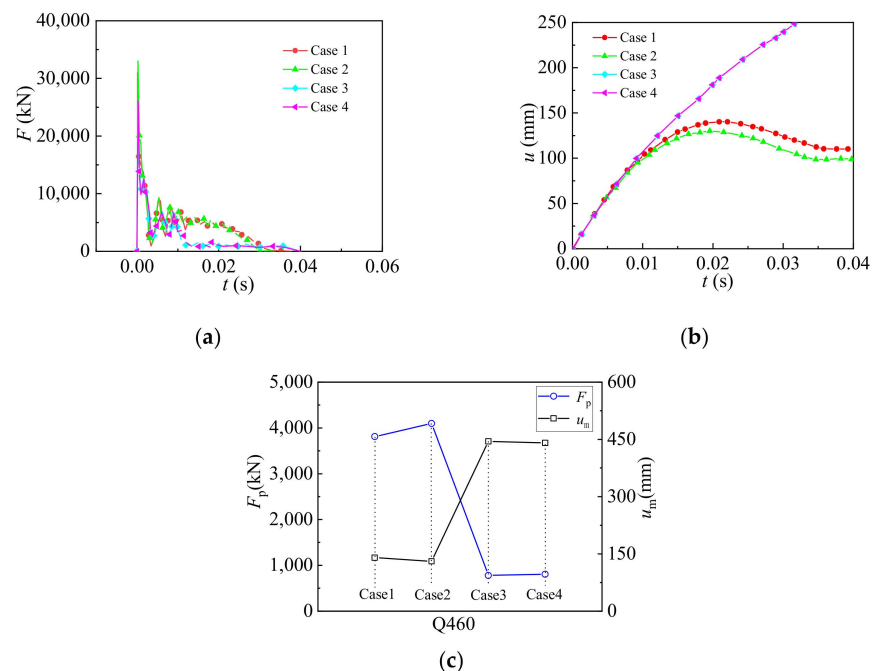

Figure 8. Comparison of Q460 steel with different dynamic constitutive models. (**a**) Comparison of impact force time-history curves of Q460 steel. (**b**) Comparison of mid-span deflection time-history curves of Q460 steel. (**c**) Platform value of impact force and maximum mid-span deflection of Q460 steel.

4.2. Comparison of Different Dynamic Constitutive Models of Concrete

Figures 9 and 10 present the effects of differences in dynamic concrete constitutive models for normal and high-strength concrete (C30, C70) in the impact force and mid-span deflection time-history curves, platform value of impact force and maximum mid-span deflection of the columns. It is observed that the effects of different concrete dynamic constitutive models are more clear for columns with high-strength concrete. The concrete dynamic constitutive model for case 2 resulted in the reduction of the platform value of

impact force with the increase in concrete strength, thus increasing mid-span displacement and deformation. The model in case 3 was in good agreement with the analysis results of the model in case 1 for the impact process. It should be noted that the strain rate effect of steel was still considered in both models; however, the strain rate effect was not considered for the concrete for case 3. The impact energy of CFST members under impact load was mainly absorbed by the outer steel tube, and its absorption rate reached more than four times that of concrete [1]. Thus, even if the strain rate effect was not considered for the concrete, the calculated results of the model in case 3 were still consistent with the actual model in case 1. However, the model in case 4 did not consider the strain rate effect of either steel or concrete, resulting in the slightly larger mid-span displacement and slightly smaller platform value of impact force.
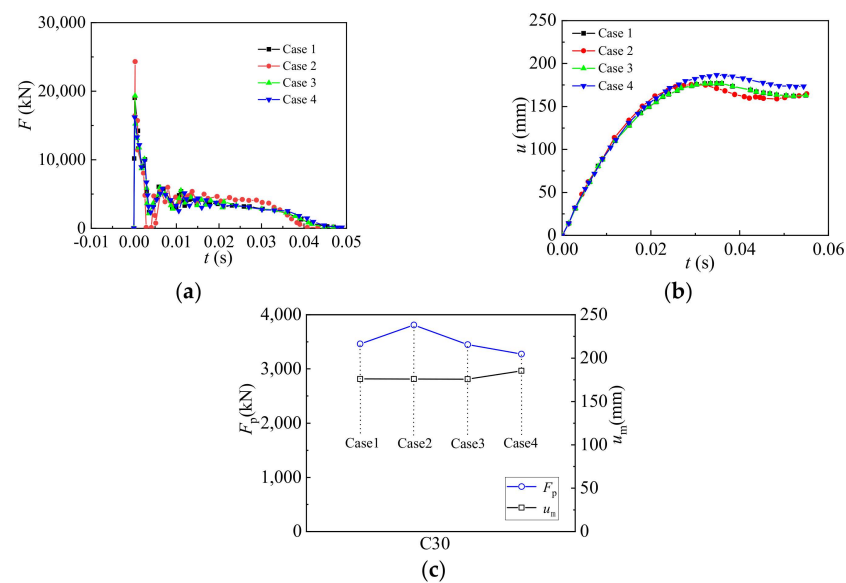
Figure 9. Comparison of C30 concrete with different dynamic constitutive models. (**a**) Comparison of impact force time-history curves of C30 concrete. (**b**) Comparison of mid-span deflection time-history curves of C30 concrete. (**c**) Platform value of impact force and maximum mid-span deflection of C30 concrete.
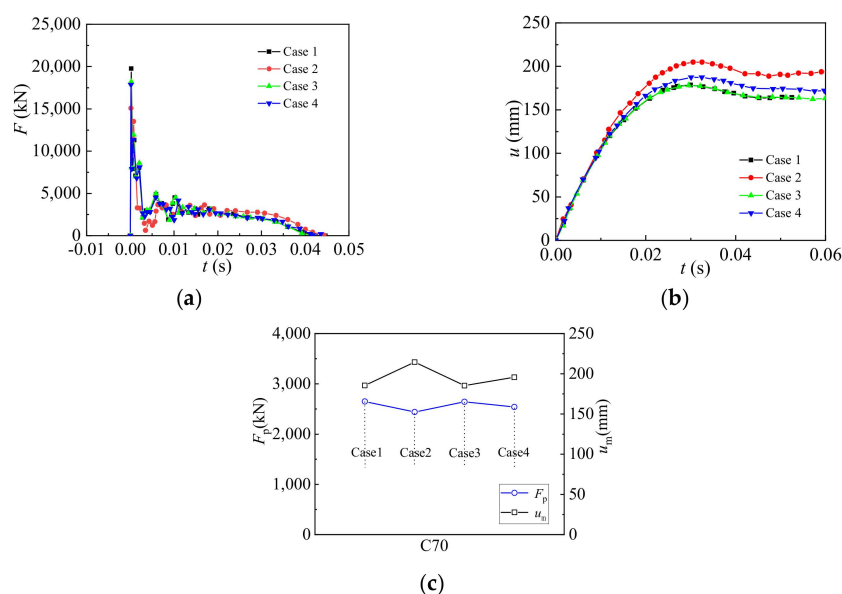
Figure 10. Comparison of C70 concrete with different dynamic constitutive models. (**a**) Comparison of impact force time-history curves of C70 concrete. (**b**) Comparison of mid-span deflection time-history curves of C70 concrete. (**c**) Platform value of impact force and maximum mid-span deflection of C70 concrete.

5. Conclusions

A comprehensive numerical study on the effects of different dynamic constitutive models of concrete and steel on the impact response of CFST columns was conducted and presented in this paper. The following conclusions can be drawn within the scope of this study:

(1) The established FE model considering the progressive damage of steel and concrete can accurately estimate the dynamic mechanical properties and failure modes of CFST columns, and thus can be used for impact response analysis of CFST members.

(2) The different dynamic constitutive models of steel have different effects on the impact force and mid-span displacement curves at the shock section of CFST columns.

(3) The FE models not considering the strain rate effect of steel have no strain rate hardening effect on the impact process. As a result, the platform value of the impact force of CFST columns is reduced and the maximum mid-span deflection is increased.

(4) The predicted result of the FE model ignoring the strain rate effect of concrete but considering the strain rate effect of steel is in good agreement with that considering the CEB–FIP model for the impact process. This is because the largest proportion of the impact energy of CFST members is mainly assimilated by the outer steel tube.

References

1. Gao, S.; Xu, Y.; Zhang, S.M.; Derlatka, A. Performance of square concrete-filled steel tubular columns under repeated lateral impact. *Eng. Struct.* **2023**, *280*, 115719. [CrossRef]
2. Momeni, M.; Ali Hadianfard, M.; Bedon, C.; Baghlani, A. Damage evaluation of H-section steel columns under impulsive blast loads via gene expression programming. *Eng. Struct.* **2020**, *219*, 110909. [CrossRef]
3. Momeni, M.; Bedon, C. Uncertainty assessment for the buckling analysis of glass columns with random parameters. *Int. J. Struct. Glass Adv. Mater. Res.* **2020**, *4*, 254–275. [CrossRef]
4. Momeni, M.; Bedon, C.; Ali Hadianfard, M.; Baghlani, A. An efficient reliability-based approach for evaluating safe scaled distance of steel columns under dynamic blast loads. *Buildings* **2021**, *11*, 606. [CrossRef]
5. Momeni, M.; Beni, M.; Bedon, C.; Najafgholipour, M.; Dehghan, S.; JavidSharifi, B.; Ali Hadianfard, M. Dynamic response analysis of structures using Legendre–Galerkin matrix method. *Appl. Sci.* **2021**, *11*, 9307. [CrossRef]
6. Han, L.H.; Li, W.; Bjorhovde, R. Developments and advanced applications of concrete-filled steel tubular (CFST) structures: Members. *J. Constr. Steel Res.* **2014**, *100*, 211–228. [CrossRef]
7. Ding, F.X.; Fu, Q.; Wen, B.; Zhou, Q.S.; Liu, X.M. Behavior of circular concrete-filled steel tubular columns under pure torsion. *Steel Compos. Struct.* **2018**, *26*, 501–511.
8. Yan, X.F.; Zhao, Y.G. Compressive strength of axially loaded circular concrete-filled double-skin steel tubular short columns. *J. Constr. Steel Res.* **2020**, *170*, 106114. [CrossRef]
9. Yan, X.F.; Zhao, Y.G. Experimental and numerical studies of circular sandwiched concrete axially loaded CFDST short columns. *Eng. Struct.* **2021**, *201*, 109828. [CrossRef]
10. Deng, Y.; Tuan, C.Y.; Xiao, Y. Flexural behavior of concrete-filled circular steel tubes under high-strain rate impact loading. *J. Struct. Eng.* **2012**, *138*, 449–456. [CrossRef]
11. Wang, R.; Han, L.H.; Zhao, X.L.; Rasmussen, K.J.R. Experimental behavior of concrete-filled double steel tubular (CFDST) members under low velocity drop weight impact. *Thin-Walled Struct.* **2015**, *97*, 279–295. [CrossRef]
12. Aghdamy, S.; Thambiratnam, D.P.; Dhanasekar, M. Effects of structure-related parameters on the response of concrete-filled double-skin steel tube columns to lateral impact. *Thin-Walled Struct.* **2016**, *108*, 351–368.
13. Wang, W.Q.; Wu, C.Q.; Li, J.; Liu, Z.; Zhi, X. Lateral impact behavior of double-skin steel tubular (DST) members with ultra-high performance fiber-reinforced concrete (UHPFRC). *Thin-Walled Struct.* **2019**, *144*, 106351. [CrossRef]
14. Zhao, H.; Wang, R.; Hou, C.C.; Lam, D. Performance of circular CFDST members with external stainless steel tube under transverse impact loading. *Thin-Walled Struct.* **2019**, *145*, 106–380. [CrossRef]

15. Zhao, H.; Zhang, W.; Wang, R.; Hou, C.C.; Lam, D. Axial compression behaviour of round-ended recycled aggregate concrete-filled steel tube stub columns (RE-RACFST): Experiment, numerical modeling and design. *Eng. Struct.* **2023**, *276*, 115376. [CrossRef]

16. Qu, H.; Li, G.; Chen, S.; Sun, J.; Sozen, M.A. Analysis of circular concrete-filled steel tube specimen under lateral impact. *Adv. Struct. Eng.* **2011**, *14*, 941–951. [CrossRef]

17. Yousuf, M.; Uy, B.; Tao, Z.; Remennikov, A.; Liew, J.Y.R. Transverse impact resistance of hollow and concrete filled stainless steel columns. *J. Constr. Steel Res.* **2013**, *82*, 177–189. [CrossRef]

18. Yousuf, M.; Uy, B.; Tao, Z.; Remennikov, A.; Liew, J.Y.R. Impact behaviour of pre-compressed hollow and concrete-filled mild and stainless steel columns. *J. Constr. Steel Res.* **2014**, *96*, 54–68. [CrossRef]

19. Han, L.H.; Hou, C.C.; Zhao, X.L.; Rasmussen, K.J. Behaviour of high-strength concrete filled steel tubes under transverse impact loading. *J. Constr. Steel Res.* **2014**, *92*, 25–39. [CrossRef]

20. Cai, J.; Yu, Y.; Chen, Q.J.; Li, Y.; Ye, J. Parameter study on dynamic response of concrete filled square tube under lateral impact. *J. Cent. South Univ. (Sci. Technol.)* **2019**, *50*, 409–419.

21. Yang, X.; Yang, H.; Zhang, S. Transverse impact behavior of high-strength concrete-filled normal-/high-strength square steel tube columns. *Int. J. Impact Eng.* **2020**, *139*, 103512. [CrossRef]

22. Yang, X.; Zhu, Y.; Yang, H.; Zhang, S. Investigations on CFST against lateral impact loading by FEA when employing rate-dependent models for different steel grades. *J. Build. Struct.* **2019**, *40* (Suppl. S1), 370–377.

23. ABAQUS. *User's Manual Version 6.14*; Dassault Systèmes: Waltham, MA, USA, 2014.

24. Han, L.H.; Yao, G.H.; Zhao, X.L. Tests and calculations for hollow structural steel (HSS) stub columns filled with self-consolidating concrete (SCC). *J. Constr. Steel Res.* **2005**, *61*, 1241–1269. [CrossRef]

25. *ACI 318-19*; Building Code Requirements for Structural Concrete and Commentary. ACI: Farmington Hills, MI, USA, 2019.

26. Cowper, G.R.; Symonds, P.S. *Strain-Hardening and Strain-Rate Effects in the Impact Loading of Cantilever Beams*; Brown University: Providence, RI, USA, 1957.

27. Johnson, G.R.; Cook, W.H. A constitutive model and data for metals subjected to large strains, high strain rates, and high temperatures. In Proceedings of the 7th International Symposium on Ballistics, Den Haag, The Netherlands, 19–21 April 1983; pp. 541–547.

28. Comite Euro-International du Beton. *CEB-FIP Model Code 1990*; Redwood Books: Trowbridge, UK, 1993.

29. Yang, Y.F.; Zhang, Z.C.; Fu, F. Experimental and numerical study on square RACFST members under lateral impact loading. *J. Constr. Steel Res.* **2015**, *11*, 43–56. [CrossRef]

30. Hou, C.C. *Study on Performance of Circular Concrete-Filled Steel Tubular (CFST) Members under Low Velocity Transverse Impact*; Tsinghua University: Beijing, China, 2012.

31. Wang, R. *Study on Dynamic Response and Damage Failure of Concrete-Filled Steel Tube under Lateral Impact*; Taiyuan University of Technology: Taiyuan, China, 2008.

32. Yang, X. *Dynamic Constitutive Models of Structural Steels and Transverse Impact Resistance of High-Strength Concrete-Filled Steel Tubes with Square Cross-Section*; Harbin University of Technology: Harbin, China, 2020.

33. Holmquist, T.J.; Johnson, G.R.; Cook, W.H. A computational constitutive model for concrete subjected to large strains, high strain rates, and high pressures. In Proceedings of the 14th International Symposium on Ballistics, Quebec, QC, Canada, 26–29 September 1993; pp. 591–600.